Nuclear Magnetic Resonance Study of the Keto–Enol Equilibrium of 3-Hydroxy-2,4-dimethylcyclobutenone

James S. Chickos,* David W. Larsen, and Larry E. Legler[1]

Contribution from the Department of Chemistry, University of Missouri at St. Louis, St. Louis, Missouri 63121.
Received September 18, 1971

Abstract: The nmr spectrum of 3-hydroxy-2,4-dimethylcyclobutenone (**1**) has been examined as a function of temperature in the range 30 to 115°. The high-temperature spectrum in water consists of a slightly broadened singlet; at room temperature the spectrum consists of two doublets of equal intensity. Analysis of the spectral line shapes for both the methyl and methine protons and ^{18}O studies suggest that the equilibration process observed in the nmr proceeds by way of 2,4-dimethylcyclobutanedione. Activation parameters of 19 kcal ($\Delta F^{\ddagger}$), 13.5 kcal (E_a), 12.8 kcal ($\Delta H^{\ddagger}$), and −16 eu ($\Delta S^{\ddagger}$) were calculated for this process.

For some years[2-5] 3-hydroxy-2,4-dimethylcyclobutenone (**1**) and related compounds have enjoyed the attention of several research groups. Cyclobutane-1,3-dione (**2**) has been reported to exist in equilibrium with its enol form in polar media,[4] while the equilibrium in methyl-1,3-cyclobutanedione (**3**) appears to lie heavily in favor of the enol.[5] In this paper we wish to report the results of our investigations concerning the nature of the keto–enol equilibrium in **1**.

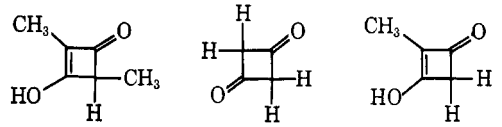

1 **2** **3**

Results and Discussion

The nmr spectrum of **1** at room temperature is shown in Figure 1. In water the methyl region consists of two doublets centered at τ 8.9 and 8.58. Both methyl groups are spin coupled to the methine proton with coupling constants of 7.0 and 2.5 Hz, respectively. As reported earlier by Farnum and coworkers,[3a] heating **1** in 10% solutions of potassium carbonate in deuterium oxide resulted in the disappearance of all resolved coupling. We have in addition found that simply dissolving **1** in deuterium oxide is sufficient to incorporate deuterium in the methine position. When **1** was dissolved in a mixture of dimethyl-d_6 sulfoxide and D_2O, the methine hydrogen was completely exchanged before the spectrum could be recorded (40 sec, 31°). Assuming a pseudo-first-order reaction, a *minimum* rate constant, k_{ex}, of 0.07 sec^{-1} (31°) is obtained. Similar results were obtained in aqueous solutions of dimethylformamide, acetonitrile, and dioxane. The exchange rate was considerably slower in an alkaline medium.[3a] The rapidity with which **1** exchanged the methine proton suggested the possibility of measuring this exchange process by standard variable temperature nmr techniques.

When aqueous solutions of **1** are heated, significant changes in lineshape occur as shown in Figure 2. These changes were found to be dependent only on the temperature and independent of the concentration of **1** over a sixfold dilution. Cooling the solutions regenerated the room temperature spectrum. Above 80° diethyl ketone was rapidly formed. As seen in Figure 2, the methyl group of diethyl ketone appears as a triplet centered at a slightly higher field than the upfield doublet of **1**, and as such did not substantially interfere with the analysis. The presence and concentration of this substance had no noticeable effect on the observed lineshapes.

The collapse of the room temperature spectrum to what appears to be a singlet at elevated temperatures can be explained as the result of some dynamic process leading to an interconversion of the two methyl groups. The mathematical expression describing the effects of exchange on nmr lineshapes has been described. Our analysis is based on solution of the lineshape equations derived by Anderson and modified by the Kubo–Sack matrix treatment under conditions of nonsaturation and slow passage.[6,7]

The line intensity at frequency ω is given by

$$I(\omega) \propto \mathrm{Re}\mathbf{W}\cdot(i\omega\mathbf{E}_n - i\Omega + 1/T_2\mathbf{E}_n - \pi)^{-1}\cdot\mathbf{A}$$

where **W** is a row vector with elements proportional to occupation probabilities of the sites in equilibrium, **A** is a column vector with all components equal to unity, $\mathbf{E}_n$ is the unit matrix of order n, Ω is a diagonal matrix with elements ω_j (Lamor frequencies for the n sites), and π is a matrix with elements $\pi_{jk} = p_{kj}$ and $\pi_{jj} = -\Sigma p_{jk}$ ($j \neq k$) where p_{jk} is the transition probability between site j and site k. T_2 is the transverse relaxation time. An experimental value of $T_2 = 0.636$ sec/radian (slow exchange limit) was used for all the calculations.

There are three distinctly different processes which can lead to changes in lineshape. Each of the sites in Figure 1 (sites 1–4) may exchange with any of the other sites, two of the other sites, or only one other site. Fig-

(1) National Science Foundation Undergraduate Research Participant, summer 1970.

(2) R. B. Woodward and G. Small, Jr., *J. Amer. Chem. Soc.*, **72**, 1297 (1950).

(3) (a) D. G. Farnum, M. A. T. Heybey, and B. Webster, *ibid.*, **86**, 673 (1964); (b) D. G. Farnum, J. R. Johnson, R. E. Hess, and B. Webster, *ibid.*, **87**, 5191 (1965); (c) D. G. Farnum, M. A. T. Heybey, and B. Webster, *Tetrahedron Lett.*, 307 (1963).

(4) (a) H. H. Wasserman and E. V. Dehmlow, *J. Amer. Chem. Soc.*, **84**, 3787 (1962); *Tetrahedron Lett.*, 1031 (1962); (b) F. A. Miller, F. E. Kiviat, and I. Matsubara, *Spectrochim. Acta, Part A*, **24**, 1523 (1968).

(5) R. B. Johns and A. B. Kriegler, *Aust. J. Chem.*, **17**, 765 (1964).

(6) P. W. Anderson, *J. Phys. Soc. Jap.*, **9**, 316 (1954); R. A. Sack, *Mol. Phys.*, **1**, 163 (1958); R. Kubo, *Nuovo Cimento Suppl.*, **6**, 1063 (1958).

(7) For an example of a similar analysis, see G. M. Whitesides and J. S. Fleming, *J. Amer. Chem. Soc.*, **89**, 2855 (1967).

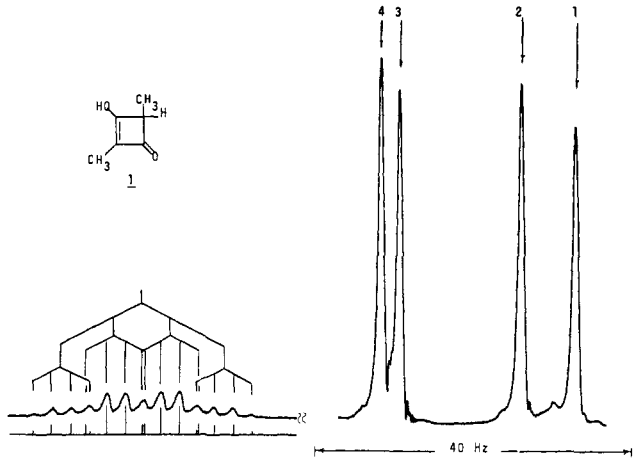

Figure 1. The room temperature nmr spectrum of **1** in dimethyl-d_6 sulfoxide (91 mg of **1**, 377 mg of DMSO-d_6). The methine hydrogen is split into 16 lines, 13 of which can be resolved by the spectrometer (60 MHz).

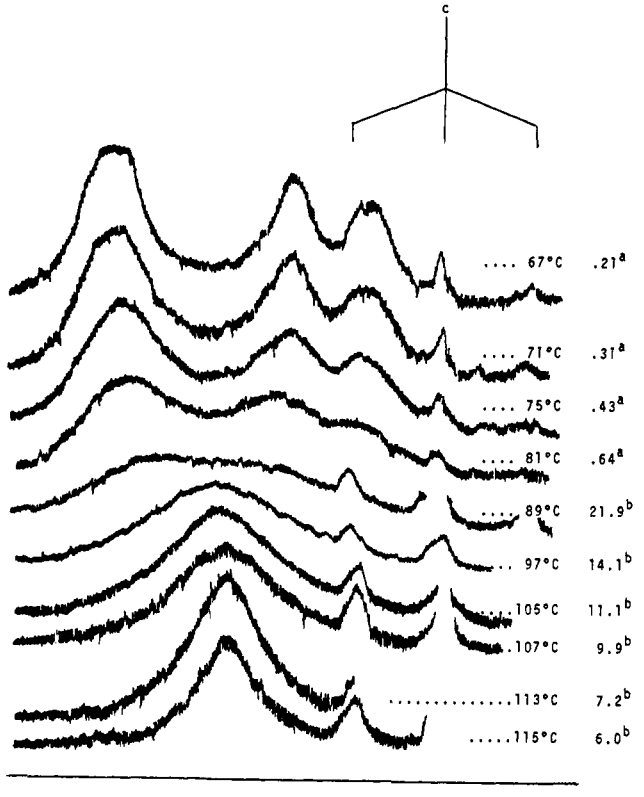

Figure 2. The temperature dependent nmr spectrum of **1** in water: a, trough to peak ratio; b, width at half height; c, diethyl ketone formed from the decomposition of **1**.

ures 3–8 summarize the results of our calculations. Figure 3, for example, illustrates a case where all sites are allowed to scramble. The spectra in this case were realized by allowing each site to exchange with all the others (all P_{jk}'s equal). An example of a mechanism which would be consistent with this mathematical model

Scheme I

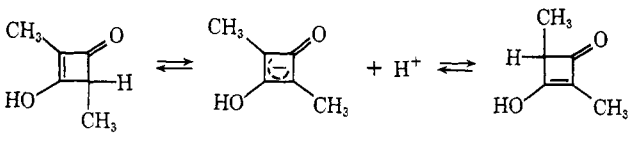

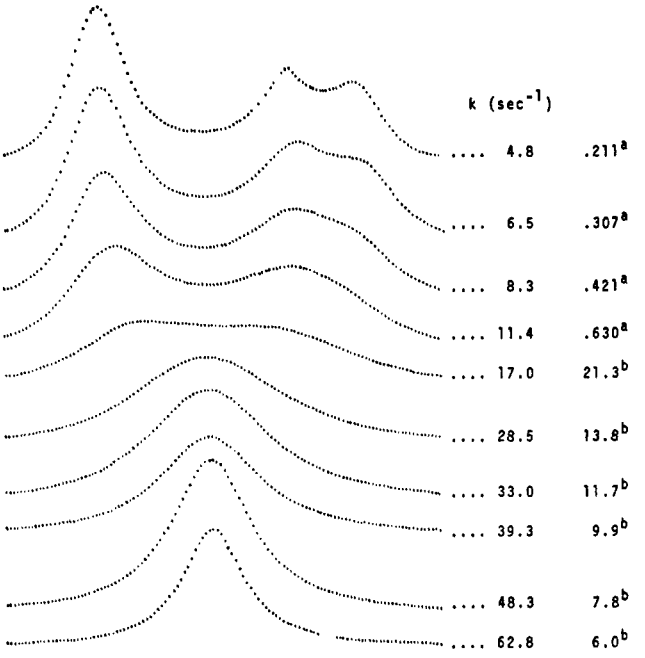

Figure 3. The theoretical lineshapes for a process which allows all sites to interconvert (*i.e.*, (1 and 2), (1 and 3), (1 and 4), (2 and 3), (2 and 4), and (3 and 4)): a, trough to peak ratio; b, width at half height (Hz). The rate constants are reported in terms of methyl group interconversion.

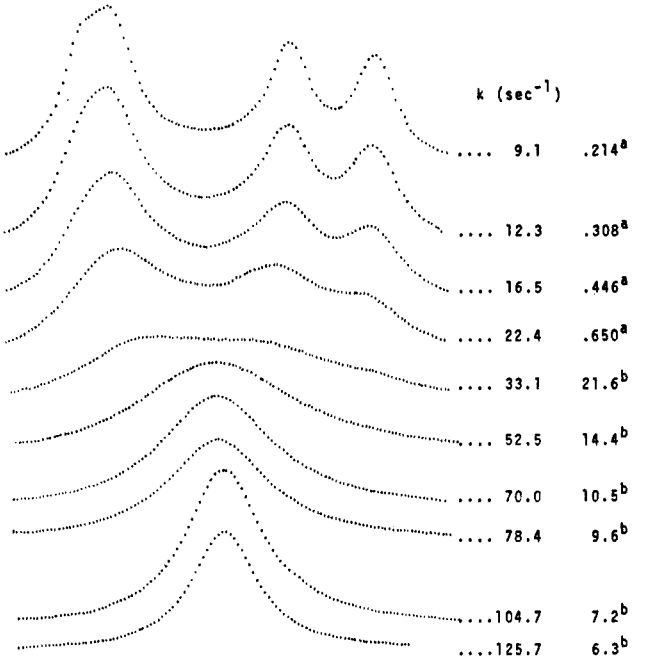

Figure 4. The theoretical lineshapes for a process which allows exchange only between sites (1 and 3), (1 and 4), (2 and 3), and (2 and 4): a, trough to peak ratio; b, width at half height. The rate constants are reported in terms of keto–enol tautomerism.

is the case where the methine proton of **1** is lost to the solvent by ionization. In the idealized case, proton capture would occur with equal probability at both allylic sites resulting in scrambling of the methyl groups and complete loss of spin memory (Scheme I).

Figures 4, 5, and 6 illustrate the cases where each site is allowed to exchange with only two other sites. In Figure 4, one site from each doublet is allowed to ex-

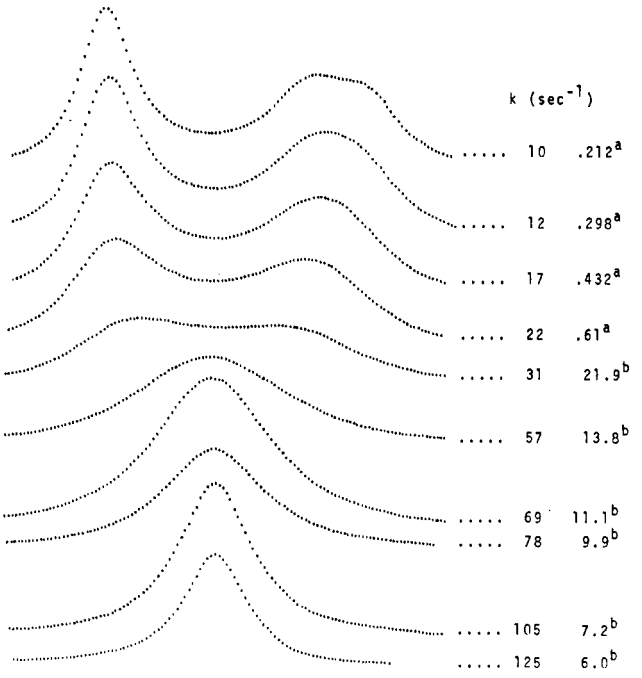

Figure 5. The theoretical lineshapes for a process which allows exchange between sites (1 and 2), (1 and 4), (2 and 3), and (3 and 4): a, trough to peak ratio; b, width at half height (Hz). The rate constants reported are for methyl group interconversion.

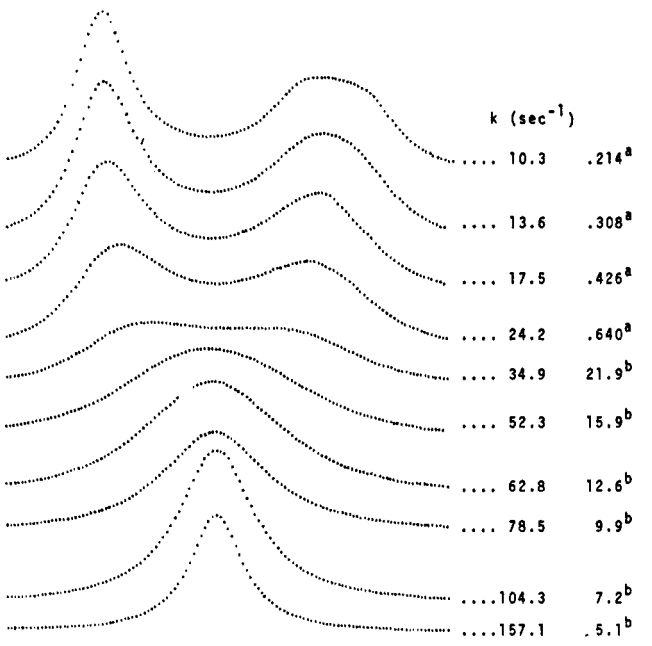

Figure 6. The theoretical lineshapes for a process which allows exchange between sites (1 and 2), (1 and 3), (2 and 4), and (3 and 4): a, trough to peak ratio; b, width at half height (Hz). The rate contants reported are for methyl group interconversion.

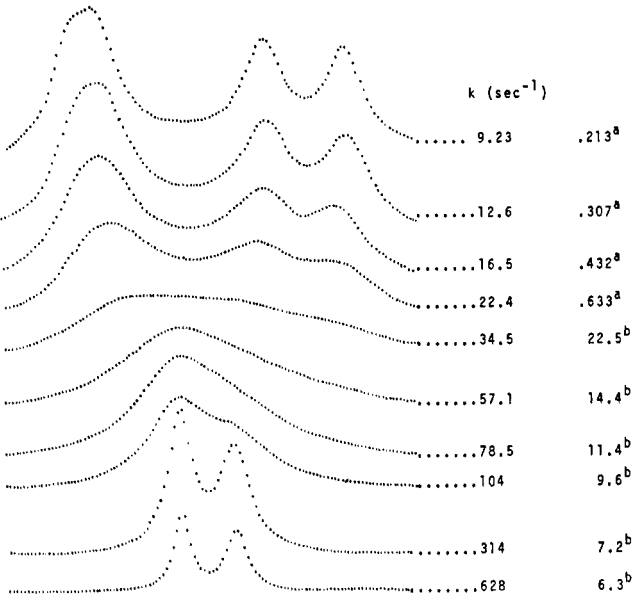

Figure 7. The theoretical lineshapes for a process which allows exchange only between sites (1 and 3) and (2 and 4): a, trough to peak ratio; b, width at half height (Hz). The rate constants reported are for methyl group interconversion.

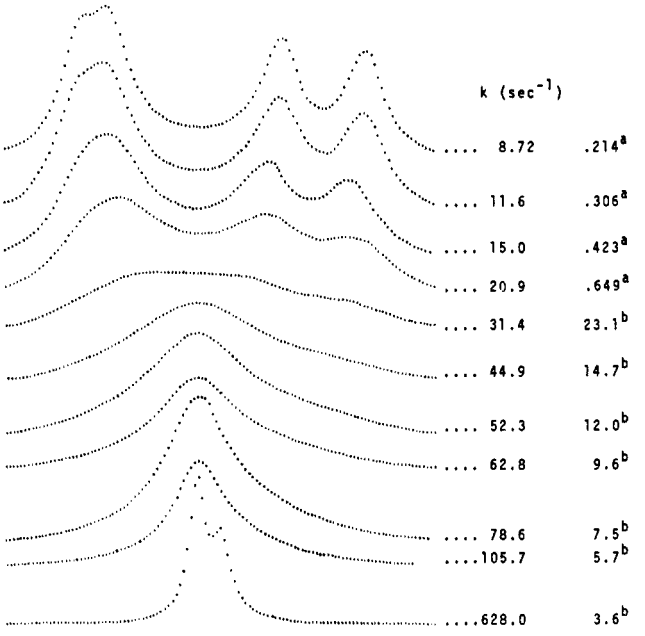

Figure 8. The theoretical lineshapes for a process which allows exchange only between sites (1 and 4) and (2 and 3): a, trough to peak ratio; b, width at half height (Hz). The rate constants reported are for methyl group interconversion.

change with the other two sites of the other doublet. Figures 5 and 6 illustrate the cases where interchange within a doublet can occur along with exchange with one site of the other doublet.

Figures 7 and 8 illustrate the last case where exchange can occur only with one other site. The trivial case where exchange occurs only within a given doublet is not shown. The line shapes for this process would be similar to those observed in the coalescence of two independent doublets. In the limit of fast exchange, each doublet would collapse to a singlet, resulting in a spectrum indistinguishable from the decoupled spectrum of **1**. Figure 7 gives the lineshapes for interchange between sites 1 and 3 and between sites 2 and 4 while in Figure 8 the inner and two outer sites are allowed to exchange.

A comparison of the calculated and observed spectra in the region of exchange broadening permits a distinction between all but two of the possibilities. Figures 3, 5, and 6 are considerably different from the experimental lineshapes in the slow exchange region.

Figure 7 differs in the fast exchange limit. Figures 4 and 8 give the best fit to the observed lineshapes within experimental error. In principle, a distinction between the processes illustrated in Figures 4 and 8 can be made at the fast exchange limit. The spectra shown in Figure 8 ultimately resolve into a doublet, while in Figure 4, a sharp singlet results. Unfortunately, the temperature required to distinguish between these two possibilities was beyond the experimentally accessible range.[8]

The mechanism which is uniquely consistent with the mathematical formulation illustrated in Figure 8 requires a [1,3] hydrogen migration with retention of the migrating group's spin state (Scheme II) and opposite signs of the coupling constants between the methine hydrogen and the two methyl groups. This allows site 1 to interconvert with site 4, and site 2 with site 3. As is apparent from a comparison of Figures 2 and 8, lineshape arguments cannot rigorously exclude this mechanism.[9]

Scheme II

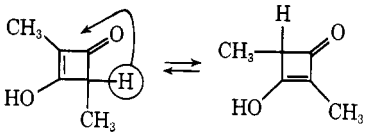

A mechanism consistent with the mathematical formulation illustrated in Figure 4 is shown in Scheme III. Interconversion of methyl groups by way of a diketone intermediate allows any site in one doublet (Figure 1) to interconvert with either site of the other doublet, depending upon the spin state of the incoming methine proton. Interconversion of spin sites within a doublet cannot be achieved by this mechanism unless the relaxation rate of the methine proton is comparable to that of keto–enol tautomerism. This possibility has previously been eliminated since the lineshapes predicted for this situation would approach those illustrated in Figure 3. Consequently, the hydrogen–deuterium exchange reaction mentioned previously and the changes in lineshape must be the results of the same dynamics process if the diketone intermediate is involved (Figure 4). Of those molecules undergoing keto–enol tautomerism only one-half of them will affect the lineshape. Molecules undergoing tautomerism in a manner which retains the original methine hydrogen do not interconvert methyl groups in enolizing. Consequently, the spin state of the methine hydrogen is unchanged and no interconversion between sites occurs. Those molecules which do lose the original methine proton during enolization affect the lineshape by interconverting methyl groups. The collapse of the original spectrum, therefore, can be explained as a result of this process.[10] Other mechanisms which do not involve a diketone intermediate but are consistent with the mathematical description illustrated in Figure 4 will be discussed below.

Scheme III

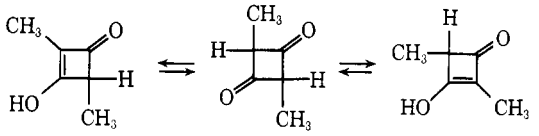

In order to distinguish between the [1,3] hydrogen shift mechanism (Figure 8) and the process described by Figure 4,[11] advantage was taken of the differences in lineshape predicted for these two processes in the fast exchange limit. The methyl doublet observed in the [1,3] hydrogen shift is a result of the effective averaging of the two methine–methyl hydrogen coupling constants.[12,13] The effect of this averaging on the nondegenerate transitions of the methine hydrogen is to reduce the expected number from 16 to 7, as shown in Figure 9a. These spectra represent the lineshapes calculated for the [1,3] hydrogen shift in the regions of slow, medium, and fast exchange (on the nmr time scale). The lineshapes were calculated by assigning the spin states for each methine hydrogen transition, 16 in all. The [1,3] hydrogen shift affects these transitions by interconverting the respective spin states of the two methyl groups. These spin state interconversions were then translated into site interconversions (assuming opposite signs in the coupling constants) and thus incorporated into the lineshape equations. Four transitions, those resulting from molecules with identical spin states in both methyl groups ($\alpha\alpha\alpha$, $\alpha\alpha\alpha$; $\beta\beta\beta$, $\beta\beta\beta$; etc.), are not affected by interconversion of spin states and hence appear as sharp transitions throughout the entire region of exchange broadening.

The lineshapes expected for the methine hydrogen undergoing rapid exchange with water are also shown in Figure 9b. The lineshapes in this case were calculated by allowing each methine hydrogen site to exchange with the water site. The mole fraction of each respective site was included in the lineshape calculations, since exchange in this case occurred between sites of different intensities. The relationships between the various lifetimes ($1/p_{jk}$) were obtained from the steady state condition. Lifetimes for each of the methine hydrogen sites and for the water site were proportional to their relative intensities.

Comparison of the lineshapes calculated for these two processes (Figure 9a,b) with those obtained experimentally in dimethyl-d_6 sulfoxide–water solutions (Figure 10) permits a distinction between the two processes. Only the hydrogen exchange process gives lineshapes in accord with those observed. Furthermore, the rate constants obtained for the methine proton exchanging

(8) Rapid evolution of carbon dioxide from decomposition of **1** was a major factor in controlling the upper temperature limit.

(9) The necessity of retaining the spin state of the methine hydrogen during migration and the rapid hydrogen–deuterium exchange reported earlier are incompatible unless hydrogen migration occurs faster than exchange.

(10) Implicit in this discussion is the assumption that the equilibrium concentration of the diketone intermediate is small, so that it makes no sizable contribution to the lineshape.

(11) Attempts to differentiate between these two mechanisms by double resonance techniques in the Hoffman–Forsen experiment were unsuccessful. Perturbations of the sites being observed (sites 3,4) by the proximity of the strong irradiating field, H_2 (at site 1), rendered the results of the experiment inconclusive. R. A. Hoffman and S. Forsen, *J. Chem. Phys.*, **39**, 2892 (1963); R. B. Larrabee, *J. Amer. Chem. Soc.*, **93**, 1510 (1971); J. Feeney and G. C. K. Roberts, *J. Chem. Soc. D*, 205 (1971).

(12) The doublet observed in the degenerate [1,2] hydride shift in the dimethylisopropylcarbonium ion is an example of an intramolecular process maintaining a similar spin memory effect in the fast exchange limit. M. Saunders, M. H. Jaffe, and P. Vogel, *J. Amer. Chem. Soc.*, **93**, 2558 (1971).

(13) The lineshapes for a [1,3] hydrogen shift occurring with similar signs in the methine–methyl coupling constants are shown in Figure 7. The coupling constants for the processes shown in Figures 7 and 8 in fast exchange limit are an average, 4.8 and 2.3 Hz, respectively.

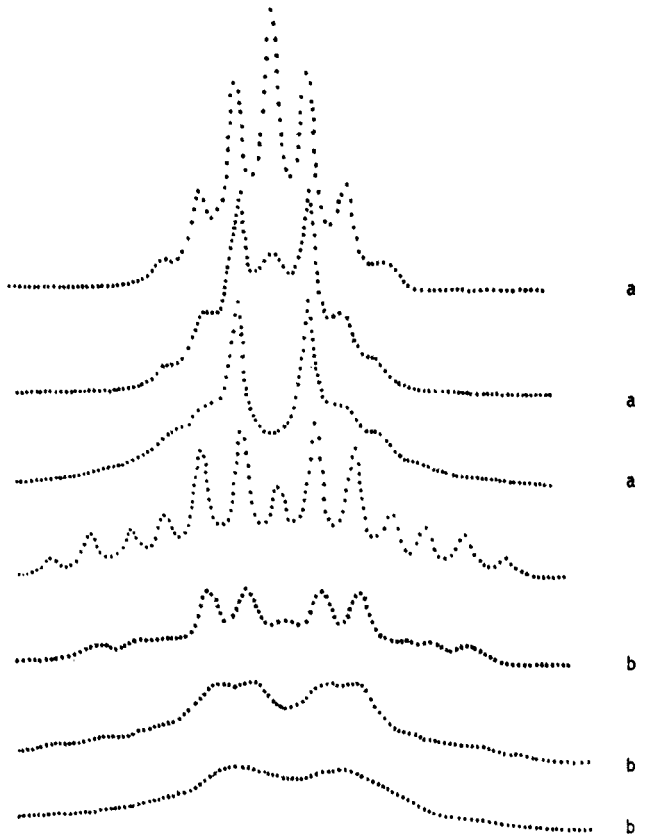

Figure 9. Theoretical lineshapes for the methine hydrogen of **1**: a, undergoing a [1,3] hydrogen shift with retention of spin and opposite signs in the two methine–methyl coupling constants; b, exchange with the water site.

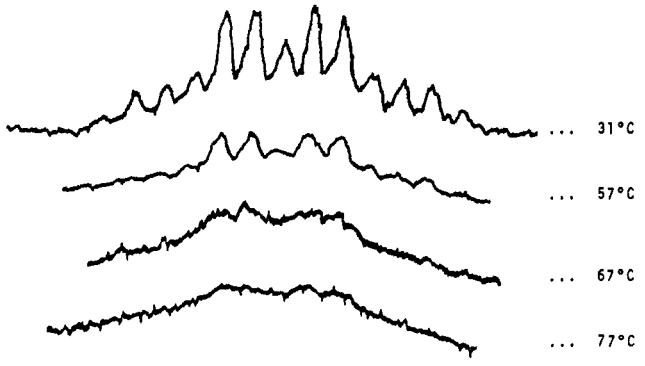

Figure 10. Methine hydrogen lineshapes as a function of temperature in dimethyl sulfoxide–water solution (91 mg of **1**, 377 mg of DMSO-d_6, 171 mg of water).

with the medium were in qualitative agreement with the rate constants obtained for methyl group interconversion. No attempt was made to obtain the best fit of experimental and calculated lineshapes, partly because of the prohibitive amount of computer time required for the calculations. The correlation between the observed and calculated lineshapes for the exchange process permits an additional restriction to the mechanistic interpretation of the process in Figure 4; the hydrogen–deuterium exchange of the methine hydrogen and changes in the lineshapes of the methyl groups must be the results of the same dynamic process.

Three mechanisms are consistent with the lineshape and hydrogen–deuterium exchange arguments advanced: the keto–enol tautomerism mechanism (Scheme III), a hydrogen transfer process proceeding through a cyclic transition state such as **4**, and a process

Figure 11. Arrhenius plot of log rate constant *vs.* reciprocal absolute temperature obtained by complete lineshape analysis for the case illustrated in Figure 4.

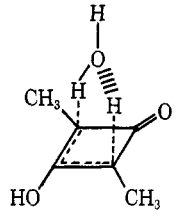

4

involving the hydration of one of the unsaturated centers of **1** in the slow step (Scheme IV). Of these

Scheme IV

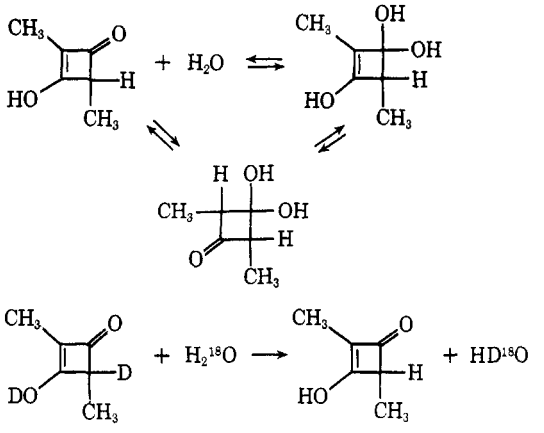

possibilities, the last is easily tested. Compound **1**, deuterated at both exchangeable positions, was dissolved in $H_2{}^{18}O$ (30 mol %) containing a small amount

of acetonitrile. After 5 min at room temperature, mass spectroscopic analysis of recovered **1** revealed the absence of deuterium without the incorporation of any detectable amount of ^{18}O. At elevated temperatures, ^{18}O was slowly incorporated. The failure to incorporate ^{18}O at a rate comparable to H/D exchange clearly eliminates this mechanism as a possibility for explaining the lineshapes observed.

Differentiation between the two remaining mechanisms on a rigorous basis is not presently possible. Of the two, the keto–enol tautomerism mechanism appears to be the most attractive. Spectroscopic detection of the diketone form, in the keto–enol equilibrium of similar compounds, is consistent with this interpretation.[4]

As mentioned previously, only one-half of the molecules undergoing keto–enol tautomerization affect the lineshapes. Consequently, a statistical factor must be introduced to convert the rates obtained from the lineshapes to rates of keto–enol tautomerism. The rates reported in Figure 4 are rates of tautomerism. The activation parameters associated with this process, $\Delta F^{\pm}$, $\Delta H^{\pm}$, and $\Delta S^{\pm}$, were calculated with the aid of the standard equations. The Arrhenius activation energy was calculated from the slope of $\ln k$ *vs.* $1/T$ plot (Figure 11). The results of these calculations are E_a = 13.5 kcal, $\log A = 9.6$ sec^{-1}, $\Delta H^{\pm} = 12.8$ kcal/mol, $\Delta S^{\pm} = -16.5$ eu, and $\Delta F^{\pm} = 18.9$ kcal/mol. For comparative purposes, an investigation of the mechanism and measurement of the activation parameters for tautomerism in both cyclobutane-1,3-dione and methylcyclobutane-1,3-dione would be of interest.

Experimental Section

Nuclear magnetic resonance spectral measurements were recorded on a Perkin-Elmer R-20 60-MHz spectrometer equipped with a variable temperature probe. Analyses were of spectra

$$I(\omega) \propto \mathrm{ReW}\cdot \begin{vmatrix} -i(\omega_1-\omega)-1/T_2-1/\tau & 0 & 1/\tau & 0 \\ 0 & -i(\omega_2-\omega)-1/T_2-1/\tau & 0 & 1/\tau \\ 1/\tau & 0 & -i(\omega_3-\omega)-1/T_2-1/\tau & 0 \\ 0 & 1/\tau & 0 & -i(\omega_4-\omega)-1/T_2-1/\tau \end{vmatrix}^{-1}\cdot \mathrm{A} \qquad (1)$$

recorded at 120-Hz sweep widths. Temperature calibration was by ethylene glycol peak separations. Room temperature spectra were also recorded on a Varian T-60 spectrometer. Mass spectra were recorded on an AEI MS 12 spectrometer. Calculations were done on an IBM 360/50 computer.

Ethoxypropyne. Ethoxypropyne was prepared in one step from β-bromovinyl ethyl ether by combining the procedures of Stork[14] and Farnum.[3a] Liquid ammonia (250 ml) was introduced into a three-necked, round-bottomed flask equipped with a mechanical stirrer, addition funnel, and Dry Ice condenser. Ferric chloride (0.13 g) and lithium metal (6.90 g, 0.986 g-atom) were added and the blue solution was stirred until formation of lithium amide was complete (*ca.* 1 hr). β-Bromovinyl ethyl ether (78.5 g, 0.52 mol) was then added over a period of 20 min. Next, methyl iodide (88.5 g, 0.623 mol) was added slowly (exothermic reaction) followed by dry ether (150 ml). The mixture was then stirred for 2 hr. Ammonium chloride (7.5 g, 0.14 mol) was introduced and the ammonia was allowed to evaporate overnight. Hydrolysis followed by extraction with ether, drying, and distillation through a short column afforded ethoxypropyne (16.6 g, 40%), boiling at 88–96° (lit.[3a] 90–92°).

3-Hydroxy-2,4-dimethylcyclobutenone (1). Compound **1** was prepared by treating propionyl chloride, triethylamine, and ethoxypropyne according to the procedure of Farnum, Heybey, and Webster.[3a]

Preparation of the Sodium Salt of 1 (5). Neutralization of an aqueous solution of **1** with sodium hydroxide to a pH of 5 followed by evaporation afforded **5** as an air stable, nonhydroscopic salt. Acidification reverted **5** back to **1**.

Sample Preparation. The concentration of **1** in most spectra varied from 0.3 to 0.6 *M* in water unless otherwise specified. The diethyl ketone formed at elevated temperatures was identified by comparison with an authentic sample of the 2,4-dinitrophenylhydrazone derivative, mp 152–154° (lit.[2] 155–156°). The diethyl ketone was separated from **1** by removal under vacuum.

^{18}O Experiment. Dissolving **1** in deuterium oxide followed by removal of the water under reduced pressure afforded **1** with 60% of the theoretical amount of deuterium in the exchangeable positions; *m/e* 112; P + 1, 28.3%; P + 2, 23.0%. Dissolved in $H_2{}^{18}O$ (33 mg, 38 mol %, ^{18}O, 5 mol % HDO) containing dimethyl sulfoxide (47 mg) at room temperature, **1**-d_2 (5.9 mg) incorporated no ^{18}O after 5 min; *m/e* 112, P + 1, 21%; P + 2, 2%. It was observed that deuterium in **1** was lost exceedingly fast in the spectrometer. Therefore **1** containing ^{18}O was prepared by heating **1**, $H_2{}^{18}O$, and dimethyl sulfoxide; *m/e* 112; P + 1, 26%; P + 2, 112%; P + 3, 18%; P + 4, 30%. This material (6 mg) was dissolved in H_2O (60 mg) containing acetonitrile (18 mg). After 5 min at room temperature the solvent was removed under vacuum; *m/e* 112; P + 1, 21.2%; P + 2, 104%; P + 3, 12.1%; P + 4, 30%.

Calculations. In the calculation of the methyl lineshapes, all the calculations are four-site cases. Each off-diagonal matrix element was zero unless a transition probability connected the two sites, in which case both elements (a_{ij}, a_{ji}) were set equal to $1/\tau$ (τ = average lifetime). The legend of each figure indicates which off-diagonal elements were set equal to $1/\tau$. For example, in Figure 7 all off-diagonal elements other than the 1,3 (3,1) and 2,4 (4,2) elements were set equal to zero resulting in the matrix in eq 1.

Calculation of the methine hydrogen lineshapes for the [1,3] hydrogen shift and exchange with water were 16- and 17-site cases, respectively. In this case the lifetimes were assigned on the basis of the steady state condition. Values for the nonzero off-diagonal elements used in these calculations are listed below. Sites were assigned on the basis of increasing τ values.

Reciprical lifetimes for the [1,3] hydrogen shift mechanism were (1,16), (16,1) = $1/\tau$; (2,13), (3,9), (4,15), (8,14), (9,3), (13,2), (14,8), (15,4) = $1/(3\cdot\tau)$; (6,11), (11,6) = $1/(9\cdot\tau)$.

Reciprocal lifetimes for exchange with water (site 1 = water site) were (2,1), (6,1), (13,1), (17,1) = $1/\tau$; (3,1), (4,1), (5,1), (9,1), (10,1), (14,1), (15,1), (16,1) = $1/(3\cdot\tau)$; (7,1), (8,1), (11,1), (12,1) = $1/(9\cdot\tau)$; (1,2), (1,3), (1,4...(1,16), (1,17) = $0.000641/\tau$.

Acknowledgments. We would like to thank the National Science Foundation for a summer undergraduate research program grant to L. E. L., the Research Corporation for partial support, the University of Missouri at St. Louis Computer Center for a generous contribution of computer time, and Professor H. Harris for running the mass spectra. Stimulating discussions with Professor R. E. K. Winter are also gratefully acknowledged.

(14) G. Stork and Maria Tomasz, *J. Amer. Chem. Soc.*, **86**, 471 (1964).